ACADEMIC PRESS

Available online at www.sciencedirect.com

SCIENCE DIRECT®

DEVELOPMENTAL BIOLOGY

Developmental Biology 258 (2003) 419–431

www.elsevier.com/locate/ydbio

c-*jun* regulation and function in the developing hindbrain

Fatima Mechta-Grigoriou,[a,*] Francois Giudicelli,[b] Cristina Pujades,[b,1] Patrick Charnay,[b] and Moshe Yaniv[a]

[a] *Unité "Expression génétique et maladies", CNRS URA 1644, Institut Pasteur 25, rue du Docteur Roux, 75724 Paris Cedex 15, France*
[b] *Unité 368 INSERM, Ecole Normale Supérieure 46, rue d'Ulm, 75230 Paris Cedex 05, France*

Received for publication 5 August 2002, revised 25 February 2003, accepted 25 February 2003

Abstract

Hindbrain development is a well-characterised segmentation process in vertebrates. The bZip transcription factor MafB/kreisler is specifically expressed in rhombomeres (r) 5 and 6 of the developing vertebrate hindbrain and is required for proper caudal hindbrain segmentation. Here, we provide evidence that the mouse protooncogene c-*jun*, which encodes a member of the bZip family, is coexpressed with *MafB* in prospective r5 and r6. Analysis of mouse mutants suggests that c-*jun* expression in these territories is dependent on MafB but independent of the zinc-finger transcription factor Krox20, another essential determinant of r5 development. Loss- and gain-of-function studies, performed in mouse and chick embryos, respectively, demonstrate that c-Jun participates, together with MafB and Krox20, in the transcriptional activation of the *Hoxb3* gene in r5. The action of c-Jun is likely to be direct, since c-Jun homodimers and c-Jun/MafB heterodimers can bind to essential regulatory elements within the transcriptional enhancer responsible for *Hoxb3* expression in r5. These data indicate that c-Jun acts both as a downstream effector and a cofactor of *MafB* and belongs to the complex network of factors governing hindbrain patterning.

Keywords: c-*jun*; *MafB/kreisler*; *Hoxb3*; *Krox20*; Rhombomere; Segmentation

Introduction

Development of the vertebrate hindbrain involves a transient segmentation process along the anteroposterior (AP) axis leading to the formation of seven to eight morphological units termed rhombomeres (r) (Lumsden and Keynes, 1989; Lumsden and Krumlauf, 1996; Wingate and Lumsden, 1996). This subdivision defines the metameric pattern of neuronal specification (Lumsden and Keynes, 1989; Clarke et al., 1998), underlies the pathways of neural crest cell migration into the branchial arches, and participates in its patterning (Lumsden et al., 1991; Serbedzija et al., 1992; Birgbauer et al., 1995; Kulesa and Fraser, 2000; Trainor and Krumlauf, 2000; Trainor et al., 2002; Ghislain et al., 2003) and in craniofacial morphogenesis. The rhombomeres constitute units of cell lineage restriction (Fraser et al., 1990; Birgbauer and Fraser, 1994) and domains of specific gene expression. Several genes, including *Hox* genes, exhibit spatially restricted expression patterns along the AP axis, the limits of which correspond to rhombomere boundaries (reviewed in Lumsden and Krumlauf, 1996; Rijli et al., 1998). Gene inactivation and ectopic expression experiments have indicated that some of these genes play important roles in the control of hindbrain segmentation and rhombomere AP specification (Gendron-Maguire et al., 1993; Rijli et al., 1993; Zhang et al., 1994; Alexandre et al., 1996; Barrow and Capecchi, 1996; Goddard et al., 1996; Studer et al., 1996; Gavalas et al., 1997; Schneider-Maunoury et al., 1997, 1998; Helmbacher et al., 1998). Among the genes involved in defining the rhombomeric territories, the transcription factors Krox20 and MafB/kreisler have been shown to directly regulate the segmental transcription

* Corresponding author. Fax: +33-1-40-61-30-33.
E-mail address: fmechta@pasteur.fr (F. Mechta-Grigoriou).
[1] Present address: Unitat de Biologia del desenvolupament, Dept. Ciéncies Experimentals i de la Salut, Universitat Pompeu Fabra, Dr Aiguader 80, 08003 Barcelona, Spain.

0012-1606/03/$ – see front matter © 2003 Elsevier Science (USA). All rights reserved.
doi:10.1016/S0012-1606(03)00135-0

of several *Hox* genes (Sham et al., 1993; Nonchev et al., 1996; Manzanares et al., 1997, 1999a, 2002; Giudicelli et al., 2001; Giudicelli et al., 2003).

Krox20 is expressed in two transverse stripes that predict and subsequently coincide with r3 and r5 (Wilkinson et al., 1989a). *Krox20* inactivation causes a change in the identity of r3 and r5 territories, resulting in the elimination of these rhombomeres and the corresponding neuronal populations (Schneider-Maunoury et al., 1993, 1997; Swiatek and Gridley, 1993; Jacquin et al., 1996; Voiculescu et al., 2001). *MafB* is also activated in the hindbrain prior to the establishment of morphological segmentation, in prospective rhombomeres (pr) 5 and 6 (Cordes and Barsh, 1994; Eichmann et al., 1997). The *kreisler* mutation in the mouse affects the regulation of *MafB* expression and prevents its activation in pr5 and pr6 (Frohman et al., 1993). This leads to a loss of morphological segmentation in the r4–r7 region and to early mis-specification of the r5–r6 territory. This hindbrain region, called rX in the mutant, lacks r5 markers but retains several r6 properties (Frohman et al., 1993; McKay et al., 1994; Manzanares et al., 1999b).

The MafB protein belongs to the Maf family of bZip-containing proteins (Cordes and Barsh, 1994; Kataoka et al., 1994a). bZip proteins function as dimeric transcription factors that contain a basic DNA binding region (b) and an amphipathic dimerization domain, referred as "the leucine zipper" (Zip). The bZip regions of Maf proteins show homology with the corresponding region of members of the well-characterised transcription factor complex AP-1. AP-1 is composed of dimers formed between members of the Jun and Fos families, which include three Jun (c-Jun, JunB, and JunD) and four Fos (c-Fos, Fos-B, Fra1, and Fra2) proteins (Angel et al., 1987, 1988; Curran and Franza, 1988; Halazonetis et al., 1988; Sassone-Corsi et al., 1988; Hirai et al., 1989). The consensus DNA binding sequence of AP-1 completely matches the middle region of the Maf DNA-binding motif (Kataoka et al., 1993). As expected from these structural similarities, Jun and Fos proteins can also dimerize in vitro with several members of the Maf family, including MafB (Kerppola and Curran, 1994; Kataoka et al., 1994b).

The complexity and promiscuity of the interaction network between bZip proteins and DNA raise the possibility that multiple bZip members are involved in the same biological processes. We decided to investigate the possible involvement of c-Jun, together with MafB, in the control of caudal hindbrain development. c-Jun is involved in various cellular processes, including proliferation, apoptosis, and oncogenic transformation (for review, see Mechta-Grigoriou et al., 2001). In situ hybridisation analysis revealed that it is expressed in mouse embryos from 14.5 days postcoïtum (dpc) within the developing cartilage, gut, and central nervous system (Wilkinson et al., 1989b). However, targeted disruption of the *c-jun* gene causes embryonic lethality at 13.5 dpc indicating that the gene is expressed at earlier embryonic stages. Homozygous *c-jun*$^{-/-}$ embryos probably die from impaired hepatogenesis (Hilberg et al., 1993; Johnson et al., 1993). They exhibit extensive apoptosis in both hepatoblast and erythroblast lineages as well as malformations in the cardiac outflow tract (Eferl et al., 1999). To determine the role of c-Jun during early stages of mouse development, we examined its expression profile in early embryos. Several sites of *c-jun* expression were identified from 8 dpc, including pr5 and pr6. Analysis of the *kreisler* mutant suggested that, in those prospective rhombomeres, c-*jun* is under the control of MafB. Furthermore, a combination of loss- and gain-of function experiments revealed that c-Jun is required for the early upregulation of *Hoxb3* in pr5 and that it acts through the Kr1 and Kr2 sites in the *Hoxb3* r5-enhancer. These data provide further insights in the regulatory network of genes governing the specification of the caudal hindbrain.

Materials and methods

Mouse lines and genotyping

The *Krox20*^{lacZ} mutation was maintained in a mixed C57B16/DBA2 background. PCR genotyping of embryo yolk sac was performed as previously described (Schneider-Maunoury et al., 1993). The *kreisler (kr)* line was kindly provided by Dr J. Lewis and maintained in 129 background. Homozygous *kr* embryos were obtained by mating *kr/kr* males with heterozygous females and identified by PCR genotyping as described (Frohman et al., 1993). The *c-jun* mutant line was kindly provided by Dr. E. Wagner and maintained in a mixed C57B16/129 background. PCR genotyping of the embryos was performed as described previously (Hilberg et al., 1993). For staging of embryos, midday of the vaginal plug was considered as embryonic day 0.5.

X-gal staining, whole-mount in situ hybridisation, and immunohistochemistry on mouse embryos

Postimplantation mouse embryos were recovered at the appropriate stage (8 to 10.5 dpc) and fixed at 4°C in phosphate-buffered saline (PBS) containing 4% paraformaldehyde (PFA) for 30 min for X-gal staining or for 8 h for direct in situ hybridisation. X-gal staining was performed as described (Sham et al., 1993). Embryos were then postfixed for 8 h and dehydrated in methanol. For Phox2B labelling at 10.5 dpc, neural tubes were dissected in PBT (PBS with 0.1% Tween 20) after fixation and prior to in situ hybridisation treatment. Whole-mount embryos and dissected neural tubes were processed for in situ hybridisation as described (Wilkinson and Nieto, 1993), using digoxigenin-labelled riboprobes. RNA probes were generated by transcription of the following DNA fragments: *c-jun*, a 1.

1-kb fragment derived from the *c-jun* cDNA which does not cross-hybridise with the other *jun* mRNAs (Angel et al., 1988); *MafB*, a 1.3-kb genomic fragment (Cordes and Barsh, 1994); *Hoxb3*, a 0.7-kb *Bam*HI–*Hin*dII genomic fragment (Wilkinson et al., 1989a, 1989b); *Hoxa3*, a 0.6-kb *Hin*dIII/*Eco*RI genomic fragment (Wilkinson et al., 1989a, 1989b); and *Phox2B*, a 1.6-kb cDNA fragment (Pattyn et al., 1997). All fragments were cloned in plasmids containing T7, SP6, or T3 RNA polymerase promoters and were linearised with the appropriate restriction enzyme before in vitro transcription. Synthesis of the probes was performed in the presence of 0.5 mM ATP, 0.5 mM GTP, 0.5 mM CTP, and 0.17 mM digoxigenin–UTP (Roche). The probes were precipitated in cold ethanol containing 95 mM LiCl, and their amount and quality were subsequently checked by gel electrophoresis. Hybridised RNA probes were detected by using alkaline phosphatase-coupled antibodies (Roche; 1/2000). Labelled embryos were postfixed in 4% PFA in PBS for 2 h at 4°C. Neural tubes from 10.5-dpc embryos were cut along the dorsal midline and flat mounted under a coverslip in 80% glycerol. For sectioning, whole-mount hybridised embryos were embedded in a gelatine 15%/sucrose 7.5% containing matrix, and 10-μm transverse sections were obtained by using a cryostat. Detection of the neurofilament protein was performed as described in Helmbacher et al. (1998).

In ovo electroporation and β-galactosidase detection

Commercial fertilised eggs (Morizeau) were incubated up to stages HH10-HH12 before electroporation. Electroporation was performed as previously described (Giudicelli et al., 2001), using a BTX820 electroporator (Quantum). The following parameters were used: 10–12 pulses of 23 V and 40 ms at a frequency of 1 Hz. The concentrations of the reporter and the expression constructs were 0.5 μg/μl, and the empty vector pAdRSVSP was used to achieve a final DNA concentration of 1 μg/μl. Embryos were collected 14 h after electroporation, fixed in 4% PFA during 10 min, and stained for β-galactosidase activity for 2 h at 30°C using bluogal (Sigma) as a substrate. Embryos electroporated with GFP expression plasmid were processed sequentially for β-galactosidase detection and anti-GFP immunostaining.

Immunoprecipitation (IP) and Western blotting

The method was adapted from Cairns et al. (1994) with modifications. In brief, C 33A cells were seeded 1 day prior transfection at a density of 5×10^5 cells/100-mm-diameter culture dish in DMEM (Sigma) supplemented with 7% FCS. The medium was changed 5 h before transfection, and cells were transfected with a total of 10 μg DNA by using the calcium phosphate method (Wigler et al., 1977). Two days posttransfection, cells were harvested and dissociated in an IP buffer (20 mM NaH_2PO_4, 250 mM NaCl, 30 mM NaPPi, 0.1% Nonidet P-40, 5 mM EDTA, 5 mM dithiothreitol) in the presence of protease inhibitor cocktail (Roche). Homogenisation was obtained by pipetting up and down before centrifugation at 14,000*g* for 10 min. Debris were pelleted, and the extracts were precleared for 30 min at 4°C with 50 μl of IP-equilibrated protein A-sepharose suspension (Amersham) or protein G-sepharose (Pierce) beads, depending on the antibody used. The precleared extracts were then transferred to another 50 μl of protein A/G-sepharose solution that had been preincubated for 30 min with 3 μg of specific antiserum against c-Jun protein (Pfarr et al., 1994) or against the Flag epitope (Sigma). After at least 1 h of incubation, the beads were washed three times in IP buffer. The precipitate was eluted in Laemmli buffer, fractionated by SDS/PAGE, and transferred to nitrocellulose. The membrane was then blocked in PBS/0.1% Tween 20/10% FCS and incubated with the indicated antibodies. Enhanced chemiluminescence reagents (Amersham) were used for detection.

Electrophoretic mobility shift assays (EMSA)

C33A cells were transfected with expression vectors encoding c-Jun (Hirai et al., 1990) or MafB linked to a Flag epitope (Giudicelli et al., 2003) or both plasmids. Nuclear extracts were prepared from transfected cells as previously described (Dignam et al., 1983; Mechta et al., 1997) and used for EMSA as described in Manzanares et al. (1997) with the following modifications: 2.5 μg of nuclear extracts were preincubated with 30 ng/μl of poly(dI-dC) at room temperature for 15 min in 15 μl of a buffer containing: 20 mM Hepes, pH 7.6, 1 mM EDTA, 20 mM KCl, 5 mM DTT, 4 mM $MgCl_2$, and 100 μg/ml of BSA. The mixture was further incubated for 15 min at room temperature after adding 1 ng of labelled oligonucleotide probe. Then, 5 μl of Ficoll (25%) was added to the reaction mixture and loaded on a 6% polyacrylamide gel including 0.25× TBE. Double-stranded oligonucleotides with the following sequences were used as probes or competitors: Kr1, 5′-ACCAC-CCCC**TAAGTCA**GCAGT-3′; Kr2, 5′-ACCATT**TGCA-GAC**ACCTACAT-3′; MARE, 5′-ACCAGCTGC**TGAGT-CA**GCAGA-3′. Kr1 and Kr2 oligonucleotides span the MafB/kreisler 1 and 2 binding sites of the *Hoxb3* r5-enhancer (Manzanares et al., 1997); the MARE oligonucleotide contains a consensus MafB/kreisler (Kataoka et al., 1994b). Potential AP-1 binding sites, defined by sequence comparison with several well-known AP-1 binding sites, are indicated in bold. Oligonucleotides were labelled by klenow filling in the presence of 10 μCi of [α-^{32}P]dATP. In supershift assays, nuclear extacts were preincubated with 1 μl specific antiserum against the c-Jun protein (Pfarr et al., 1994) or the Flag epitope (Sigma).

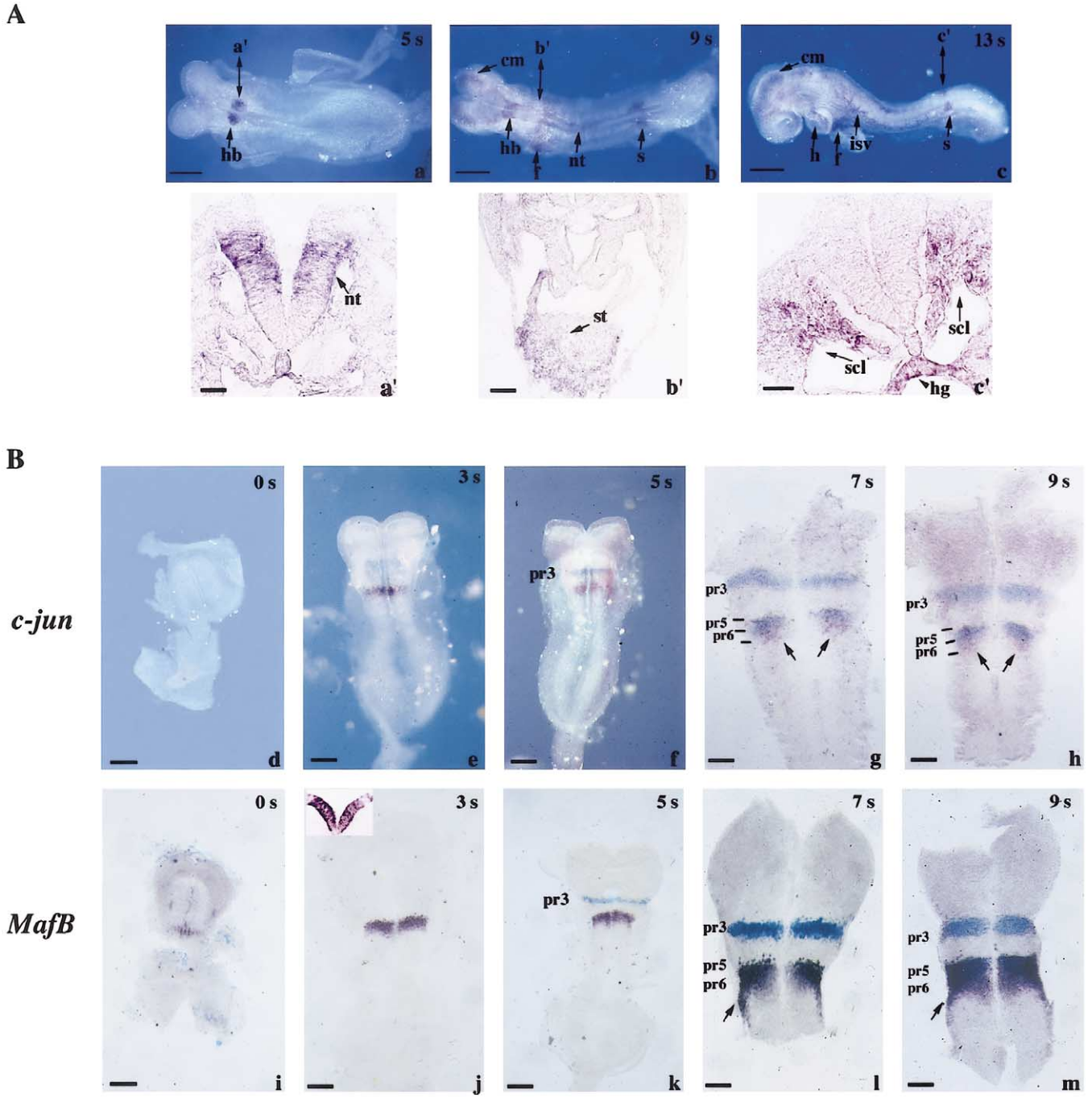

Fig. 1. (A) Whole-mount in situ hybridisations were performed by using a *c-jun* probe on wild-type embryos at the indicated somite stages. Dorsal (a, b) and lateral (c) views are shown to visualise *c-jun* labelling. (a′–c′) Transverse sections at the AP axis levels indicated by the double arrows in the above figures. cm, cephalic mesoderm; fg, foregut; h, heart; hb, hindbrain; hg, hindgut; isv, intersomitic vessels; n, neuroepithelium s, somite; scl, sclerotome; st, septum transversum. Scale bars: 60 μm (a–c) and 100 μm (a′–c′). (B) Whole-mount in situ hybridisations were performed with *c-jun* (d–h) and *MafB* (i–m) probes on embryos at the indicated somite stage. Whole mounts are shown in (d–f, i–k) and flat mounts of the hindbrain opened on the dorsal edge in (g, h, l, m). Rostral is to the top. Embryos in (f–h, k–m) carry a knock-in of *lacZ* into the *Krox20* locus and were double labelled by in situ hybridisation and X-gal staining to reveal the positions of pr3 and pr5. Arrows in (g, h) indicate that the *c-jun* expression domain extends out of the *Krox20*-positive pr5 into pr6. At the 7 and 9 s stages, *MafB* is highly expressed in pr5 and pr6 as well as in dorsal cells migrating along the neural tube at the level of r7 (arrows in 1, m). At the 7 s stage, the *MafB* expression domain is not yet sharply delimited as indicated by the presence of several indentations into pr4. pr, prospective rhombomere. Scale bars: 60 μm (d–f, i–k) and 30 μm (g, h, l, m).

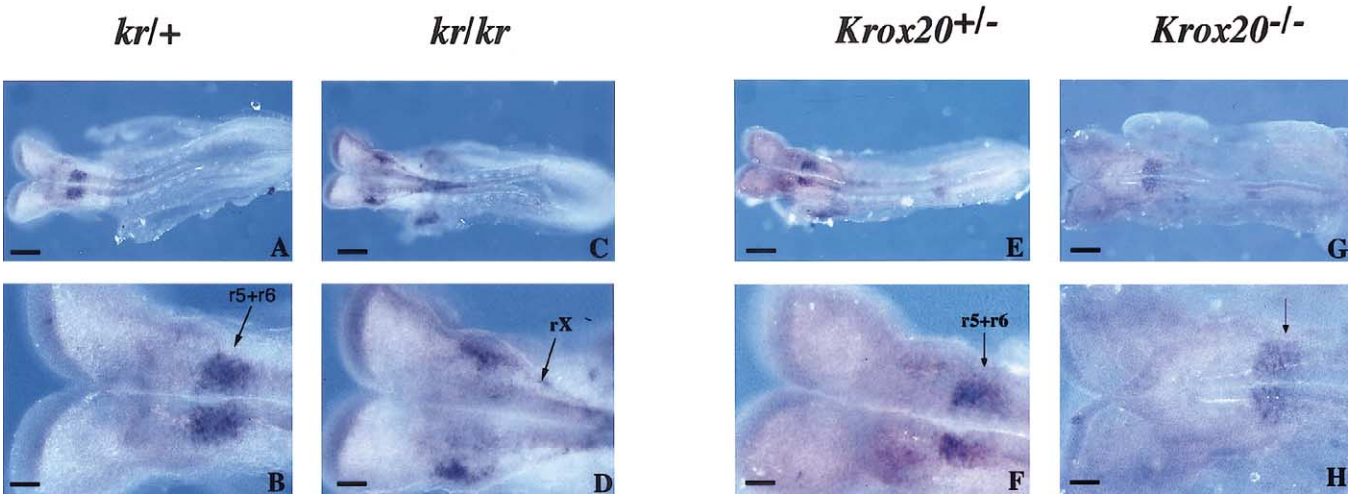

Fig. 2. MafB is required for *c-jun* expression in pr5/6. *c-jun* expression was analysed by whole-mount in situ hybridisation in 8–9 s stage embryos heterozygous or homozygous for the *kreisler* (A–D) and *Krox20* (E–H) mutations. (B, D, F, H) correspond to higher magnifications of (A, C, E, G), respectively. Embryos are oriented rostral to the left. (D) Note the absence of *c-jun* labelling in the *kr/kr* embryo at the level of rX. In contrast, *c-jun* expression is not affected by the *Krox20* mutation (E–H). Scale bars: 60 μm (A, C, E, G) and 15 μm (B, D, F, H).

Results

c-jun and MafB expression patterns overlap in the hindbrain

To gain insight into early functions of c-*jun*, we analysed its expression profile during early stages of development by whole-mount in situ hybridisation (Fig. 1A). *c-jun* expression was first observed at the beginning of somitogenesis, with strong staining initially detected in the posterior hindbrain region (Fig. 1A, a). Transverse sections along the AP axis indicated that *c-jun* expression was restricted to the middle portion of the neuroepithelium (Fig. 1A, a′). By the 8–9 s stage, the expression of *c-jun* was induced at several other sites, including more caudal regions of the dorsal neural tube, the cephalic mesoderm, the heart, the foregut, and the hindgut (Fig. 1A, b). The staining lining the posterior half of the foregut, immediately behind the heart, corresponded to the septum transversum which is involved in the outgrowth of the hepatic bud (Fig. 1A, b′) (Rossi et al., 2001). By the 12–13 s stage, *c-jun* mRNA was also detected in the intersomitic blood vessels and the developing somites. The strongest expression level was observed in the most recently formed somites (Fig. 1A, c) and corresponded to the prospective sclerotomal derivative of the somite (Fig. 1A, c′).

The expression pattern of c-*jun* in the caudal part of the developing hindbrain was reminiscent of that of *MafB* (Cordes and Barsh, 1994). We performed a detailed comparison of the pattern and timing of expression of both genes (Fig. 1B). *MafB* mRNA was first detected in the neural plate at the 0–1 s stage in a narrow stripe of cells in the caudal hindbrain, while *c-jun* expression was first observed at the 3 s stage in the same region (Fig. 1B, d, e, i, j). While *c-jun* expression was restricted to the middle portion of the neuroepithelium (Fig. 1A, a′), *MafB* expression appeared across the whole dorso/ventral extent of the neural tube (section Fig. 1B, j insert). At the 3 s stage, *c-jun* and *MafB* expression domains coincide with the prospective r5/6 region as judged by morphological landmarks (Osumi-Yamashita et al., 1996; Ruberte et al., 1997) (Fig. 1B, e, j). To confirm the precise localisation of these expression domains, we took advantage of a mouse line carrying a *lacZ* insertion in the *Krox20* locus (*Krox20*^{lacZ} allele) (Schneider-Maunoury et al., 1993). *Krox20*$^{lacZ/+}$ embryos develop normally, and *lacZ* expression faithfully recapitulates that of *Krox20* in developing r3 and r5 (Schneider-Maunoury et al., 1993). We performed double labelling experiments, using β-galactosidase activity to follow *Krox20* expression and in situ hybridisation to monitor c-*jun* and *MafB* expression. At the 5 s stage, β-galactosidase activity was essentially restricted to pr3 (Fig. 1B, f, k) (Schneider-Maunoury et al., 1993), while *c-jun* and *MafB* expression domains corresponded to pr5/6. At the 7 and 9 s stages, when *Krox20* expression was also activated in pr5, the rostral parts of the *c-jun* expression domains overlapped with the caudal *Krox20* stripe (pr5) and the caudal parts extended into pr6 (Fig. 1B, g, h). *MafB* labelling completely covered the r5-specific *Krox20* staining and also extended into pr6 (Fig. 1B, l, m). At the 9 s stage, *MafB* mRNA was detected in dorsal cells along the neural fold at the level of r7 (Fig. 1B, l, m). Beyond the 9 s stage, *c-jun* became progressively downregulated in r5 and r6, beginning at the ventral part of r6, and was no longer detected in the hindbrain after the 12 s stage (data not shown). *MafB* expression persisted up to the 20 s stage and subsequently disappeared, first dorsally and then ventrally (data not shown). In conclusion, *c-jun* is expressed in the prospective r5 and r6 territories of the

developing hindbrain with a highly dynamic pattern. Its activation immediately follows that of *MafB*, and its expression domain is always included within that of *MafB*.

c-jun expression in r5/6 requires MafB but not Krox20 activity

The respective patterns of expression of *c-jun* and *MafB* in the developing hindbrain raised the possibility that *c-jun* might lie downstream of *MafB* in a regulatory cascade. To investigate this issue, we analysed *c-jun* expression in *kreisler* mutant embryos. This mutation prevents expression of *MafB* in r5/6, and this territory is replaced by rX, which lacks r5 identity but retains some r6 markers (Frohman et al., 1993; McKay et al., 1994; Manzanares et al., 1999b). In heterozygous *kr*/+ embryos at the 8–9 s stage, *c-jun* was expressed in pr5/6 as in wild-type embryos (Fig. 2A and B). In contrast, in *kr/kr* embryos at the same stage, *c-jun* mRNA was not detectable in this region (Fig. 2C and D). Furthermore, *c-jun* expression was not observed in this region in *kr/kr* embryos at the 12 s stage, suggesting that lack of *c-jun* expression in the rX region is not due to a developmental delay in r5 (data not shown). These data suggest that MafB is required for expression of *c-jun* in pr5/6. Surprisingly, ectopic expression of *c-jun* was observed in *kr/kr* embryos within the dorsal neuroepithelium at the level of pr3/4 (Fig. 2C and D), as well as at the level of the dorsal closure of the neural tube (Fig. 2C). These domains of expression are reminiscent of the pattern of apoptotic cells in the neuroepithelium of *kr/kr* embryos (McKay et al., 1994), raising the possibility that c-Jun might be involved in this process as already observed in other systems (Bossy-Wetzel et al., 1997).

While c-*jun* is activated before *Krox20* in r5 (Fig. 1B), the expression domains of both genes overlap in this rhombomere between the 5 and 10 s stages. Since Krox20 is a key regulator of gene expression in the developing hindbrain, it might be involved in the maintenance of c-*jun* expression in r5. The *Krox20* mutation ultimately leads to the disappearance of r5. Nevertheless, there is a time window during which the presumptive r5 territory is still present (up to 9 dpc) (Schneider-Maunoury et al., 1993; Seitanidou et al., 1997; Voiculescu et al., 2001). This allowed us to analyse the expression of c-*jun* in r5 in *Krox20*$^{-/-}$ embryos. In 8 s embryos, there was no modification in the level of expression of c-*jun* or in the AP length of the positive domain as compared with heterozygous or wild-type embryos (Fig. 2E–H). This suggests that Krox20 is not involved in the control of c-*jun* expression in r5.

c-Jun is involved in the initial activation of Hoxb3 expression in r5

c-Jun being a transcription factor, its presence in the hindbrain raised the possibility that it could be involved in the control of the expression of downstream genes. In this respect, *Hoxb3* and *Hoxa3* constitute attractive candidates since: (1) *Hoxb3* is expressed throughout the posterior neural tube up to the r4/r5 rhombomere boundary, with higher levels in r5 (Wilkinson et al., 1989b; Hunt et al., 1991a; Sham et al., 1992; Seitanidou et al., 1997) and *Hoxa3* is expressed caudally to the r4/r5 rhombomere boundary (Hunt et al., 1991a; Manzanares et al., 1999a, 2001); (2) MafB, which constitutes a potential heterodimerisation partner of c-Jun, is involved in the direct transcriptional activation of *Hoxb3* in r5 and of *Hoxa3* in r5 and r6 (Manzanares et al., 1997, 1999b, 2002). We therefore investigated the consequences of *c-jun* inactivation on the expression of these genes, using a previously generated null allele (Hilberg et al., 1993). At early stages of hindbrain development (3–5 s), when *c*-Jun is normally present in pr5, c-*jun* inactivation prevented *Hoxb3* upregulation in r5, while it did not affect its expression in more caudal regions (Fig. 3A–D). In contrast, at the 8–10 s stage, when *c-jun* expression decreases in the hindbrain, r5 expression of *Hoxb3* was restored in *c-jun* mutant embryos (Fig. 3E and F) and maintained at least until the 15–16 s stage (Fig. 3G and H). Since *Hoxb3* is under the control of MafB, the action of c-Jun on *Hoxb3* might be exerted by MafB. We therefore analysed the expression of *MafB* in the c-*jun* null mutant at early stages of hindbrain segmentation. *MafB* was expressed normally in r5/r6 territory in the *c-jun* mutant (Fig. 3I and J). Moreover, c-*jun* inactivation did not affect *Hoxa3* expression in r5/6, even at early stages of hindbrain development (Fig. 3K and L). These data show that c-Jun is required for the initial activation of *Hoxb3* in r5, and that at later stages, *Hoxb3* expression becomes independent of c-Jun. In contrast, the expression of *Hoxa3* and *MafB* is always independent of c-Jun.

The delay in *Hoxb3* activation in r5 raised the possibility that *c-jun* mutation might cause a general delay in the maturation of this rhombomere. We therefore analysed the expression of other r5 markers, such as *Krox20* and *EphA4*, and observed that *c-jun* inactivation did not affect the early expression of these genes in r5 (Fig. 3M–P). These data indicate that the delay in *Hoxb3* appearance in r5 is not due to a delay in the maturation of this rhombomere.

Despite this conclusion, other genes might be affected in r5 in c-*jun* null embryos, resulting in later defects. Since neuronal differentiation in the hindbrain creates segment-specific characteristics, we monitored the rhombomeric patterns of neurogenesis by analysing the expression of the *Phox2B* gene and of the 155-kDa component of neurofilaments. *Phox2B* is normally expressed in three longitudinal columns in the hindbrain during neurogenesis, with some rhombomeric variations (Pattyn et al., 1997) (Fig. 3Q). c-*jun* inactivation did not affect the *Phox2B* expression pattern in r5 at 10.5 dpc (Fig. 3R). Similarly, neurofilament staining, which allows labelling of both cell bodies and axons, was not affected in the *c-jun* knock-out (Fig. 3S

and T). These data suggest that hindbrain neuronal differentiation is not grossly affected by the mutation.

c-Jun acts through the Hoxb3-r5 enhancer

The transcription of *Hoxb3* in r5 is controlled by an enhancer element (r5-enhancer), which has been characterised as a direct target of the MafB and Krox20 transcription factors (Manzanares et al., 1997, 1999b, 2002). We investigated the possibility that the role of c-Jun in *Hoxb3* regulation could be via the r5-enhancer. We performed in ovo electroporation experiments in the chick hindbrain, a system in which *Hoxb3* r5-enhancer activity is dependent on both MafB and Krox20 (Manzanares et al., 2002). A *lacZ* reporter construct, driven by the r5-enhancer, was coelectroporated with c-*jun* expression constructs or an empty vector (Giudicelli et al., 2001) (Fig. 4A–C). As expected, coelectroporation with the empty vector led to specific reporter expression in r5 in all electroporated embryos (Fig. 4A, and Table 1A). Coelectroporation with wild-type c-*jun* led to further activation of the *Hoxb3* enhancer over a large portion of the neural tube (Fig. 4B). This corresponded to the entire electroporated region, as indicated by the coelectroporation of a GFP marker (data not shown). X-gal staining along the neural tube apart from r5 was of moderate intensity in the most electroporated embryos (Table 1A). It was not enhanced in specific rhombomeres, in contrast to electroporations performed with *MafB* or *Krox20*, which led to strong additional activation in r3 and r6, respectively (Fig. 4D and G and Table 1, B and C). Coelectroporation of the reporter with a construct driving a mutant c-Jun, c-JunΔZip, lacking the Zip domain required for dimerisation and subsequent DNA binding (Hirai et al., 1990), did not activate the reporter gene (Fig. 4C, Table 1A).

The chick electroporation system also offers the possibility of testing cooperation between different trans-acting factors (Manzanares et al., 2002). We performed coelectroporation of the reporter construct and the c-*jun* vector together with *MafB* and *Krox20* expression constructs. Coelectroporation of c-Jun and MafB vectors showed an additive, rather than synergistic, effect (Fig. 4B, D and E, and Table 1, A and B). In contrast, coelectroporation of c-*jun* and *Krox20* expression vectors led to strong induction of the reporter in a large part of the neural tube (Fig. 4H, Table 1C). The level of reporter gene expression was significantly higher than upon electroporation of c-Jun or Krox20 alone (Fig. 4B and G, and Table 1A and C). As expected, coelectroporation with the defective c-*jun* mutant did not affect the patterns induced by *MafB* or *Krox20* expression vectors (Fig. 5F and I). Taken together, these data show that ectopic expression of c-*jun* alone is sufficient to promote *Hoxb3* enhancer activity and that coexpression with *Krox20* leads to synergistic activation of the *Hoxb3* enhancer.

c-Jun interacts with MafB and binds to the MafB/kreisler binding sites (Kr1 and Kr2) of the Hoxb3-r5 enhancer in vitro

The bZip region of Maf proteins shows high similarity with the corresponding region of AP-1 proteins, among them c-Jun. This prompted us to analyse physical interaction between c-Jun and MafB. We cotransfected expression plasmids encoding c-Jun or c-JunΔZip together with Flag-tagged MafB or JunD. JunD belongs to the AP-1 family and was used as a positive control in this experiment. The yield of transfected proteins in extracts was determined after immunoblotting with anti-Flag or anti-c-Jun antibodies (Fig. 5A, bottom). Immunoprecipitation with an anti-c-Jun antibody was followed by gel electrophoresis and Western blot analysis with the anti-Flag antibody. c-Jun was coimmunoprecipitated with MafB, whereas c-JunΔZip, which lacks the Zip domain, was not (Fig. 5A, left). The efficiency of c-Jun and MafB coimmunoprecipitation was comparable to that of the well-established c-Jun/JunD dimer (Fig. 5A). The c-Jun/MafB interaction was confirmed by the reciprocal experiment: immunoprecipitation of MafB using the anti-Flag antibody and detection of c-Jun with a specific c-Jun antibody (Fig. 5A, right). These data establish that MafB and c-Jun can form a complex in cells.

The *Hoxb3* r5-enhancer contains two blocks of sequences that are conserved between mouse and chicken, including the MafB/kreisler binding sites Kr1 and Kr2, respectively (Manzanares et al., 1997). AP-1 DNA binding motif matches the central sequence of the consensus Maf DNA-binding motif (MARE sequence) (Kataoka et al., 1994b). We investigated the possibility that c-Jun controls the activity of the *Hoxb3* r5-enhancer by direct interaction, as homodimer or heterodimer, with Kr1 and Kr2 sequences. We performed an electrophoretic mobility shift assay (EMSA) with nuclear extracts from cells transfected with plasmids encoding c-Jun and/or a Flag-tagged MafB and DNA probes corresponding to a consensus MARE or Kr sequences. c-Jun interacted with MARE with a similar efficiency as MafB, but formed complexes with different electrophoretic mobilities (Fig. 5B). In addition, an intermediate band was also observed in presence of both proteins, suggesting binding as heterodimer. Intermediate bands were also observed when only one expression plasmid was transfected and might correspond to the formation of heterodimers with endogenous bZIP proteins. The Kr1 site was bound by c-Jun as efficiently as the consensus MARE site, but a lower affinity was observed for the Kr2 sequence (Fig. 5C). To confirm the composition of the protein/DNA complexes, we performed supershift experiments using specific anti-c-Jun or anti-Flag antibodies (Fig. 5C). The anti-Jun antibody decreased AP-1/DNA complex formation (see also Mechta et al., 1997), whereas the anti-Flag generated a supershifted band. When c-Jun was overexpressed alone, we observed a major faster migrating band and a less intense intermediate band. Both bands almost completely disappeared in

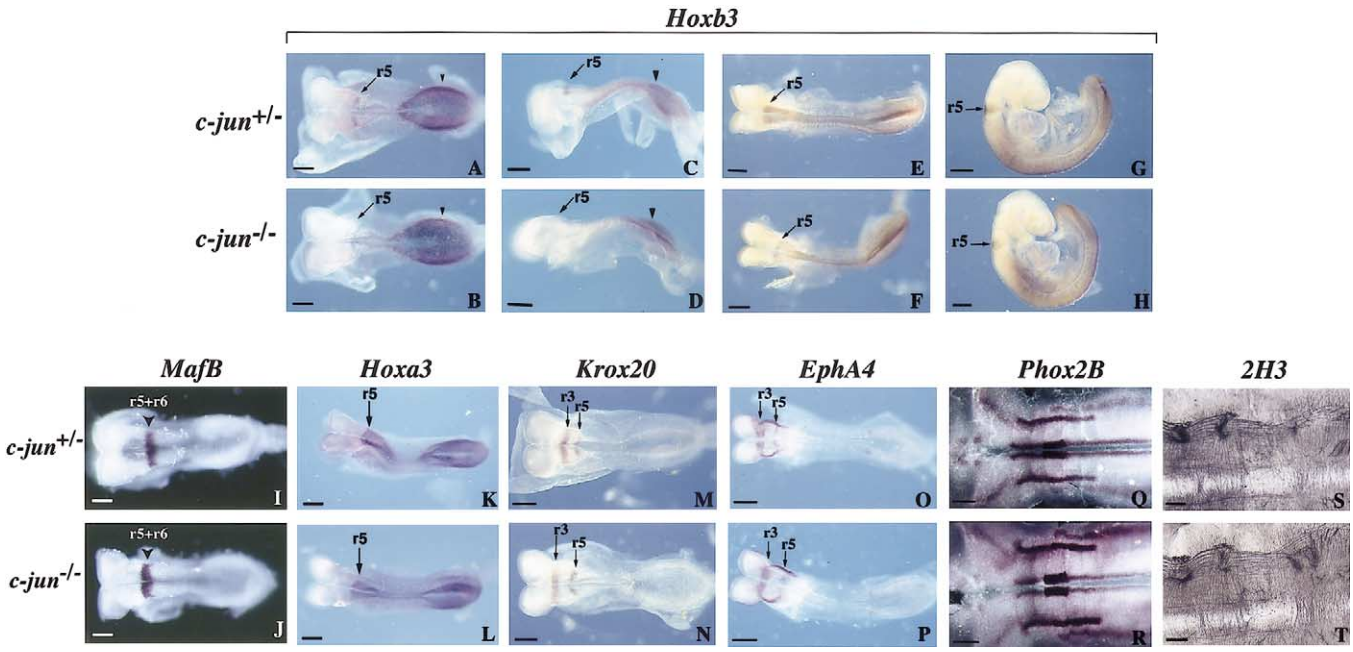

Fig. 3. c-Jun is required for *Hoxb3* early upregulation in r5. Embryos heterozygous (A, C, E, G) or homozygous (B, D, F, H) for the c-*jun* mutation were analysed for *Hoxb3* expression by whole-mount in situ hybridisation (A, B, 3–4 s stage; C, D, 5–6 s stage; E, F, 9–10 s stage; and G, H, 15–17 s stage). Embryos heterozygous (I, K, M, O, Q, S) and homozygous (J, L, N, P, R, T) for the *c-jun* mutation were analysed by in situ hybridisation for expression of *MafB* (I, J, 3–4 s stage), *Hoxa3* (K, L, 7–8 s stage), *Krox20* (M, N, 6–7 s stage), *EphA4* (O, P, 7–8 s stage), and *Phox2B* (Q, R, 10.5 dpc) and by immunochemistry with the 2H3 antibody directed against the 155-kDa component of neurofilaments (S, T). While expression of the other analysed markers was not affected by the *c-jun* mutation, the early activation of *Hoxb3* in r5 was prevented. The more caudal expression of this gene was not affected (arrowhead in A–D). Scale bars: 60 μm.

the presence of the c-Jun antibody, indicating that they both contain the c-Jun protein. When MafB was overexpressed, we observed an increase in the intensity of the intermediate band and a slower migrating band appeared. These two complexes were supershifted by addition of the anti-Flag antibody, suggesting that MafB was present in these complexes. Finally, when c-Jun and MafB were coexpressed, the intensity of the three (slow, intermediate, and fast) retarded complexes increased. Addition of anti-c-Jun or anti-Flag antibodies suggested that the faster migrating band corresponds to c-Jun homodimers, the intermediate to c-Jun/MafB heterodimers, and the slower band to MafB homodimers. Addition of anti-c-Jun and anti-Flag antibodies together almost completely displaced the three retarded bands, confirming that c-Jun and MafB are the main components of the bound complexes.

Discussion

The developing hindbrain constitutes one of the best understood regions of the CNS in terms of regional specification. Extensive genetic studies in recent years have unravelled a network of growth factors, receptors, and transcription factors that regulate the segmentation process in this embryonic territory. In the present study, we investigate the role of bZip proteins in the hindbrain patterning.

c-jun regulation in the developing hindbrain

We found that c-*jun* expression within r5 and r6 follows *MafB* induction and that its domain of expression is always included within that of *MafB*. Furthermore, the *kreisler* mutation prevents c-*jun* activation. Although we cannot exclude that *c-jun* expression is missing because of the early loss of r5 and partial reprogrammation of r6 in *kr/kr* embryos, these data suggest that c-*jun* lies downstream of MafB in a regulatory cascade acting in r5 and r6. In contrast, the control of c-*jun* expression appears not to require Krox20. The characteristics of c-*jun* regulation in r5/r6 resemble those of *Hoxa3*, which is expressed in r5 and r6 and is controlled by a *cis*-acting element, an r5/r6 enhancer. This enhancer is bound by MafB, but is independent of Krox20 (Manzanares et al., 1999a). Despite these similarities, we do not know whether MafB is a direct transciptional activator of c-*jun* transcription.

While *c-jun* expression is restricted to the middle portion of the neuroepithelium, *MafB* expression extends across the whole dorsoventral axis of the neural tube. Moreover, although the c-*jun* expression pattern in the hindbrain initially mimics that of *MafB*, they diverge beyond the 9 s stage. At this stage, c-*jun* is progressively downregulated, while *MafB* expression is maintained until the 20 s stage. Persistent expression of MafB is not sufficient to maintain *c-jun*

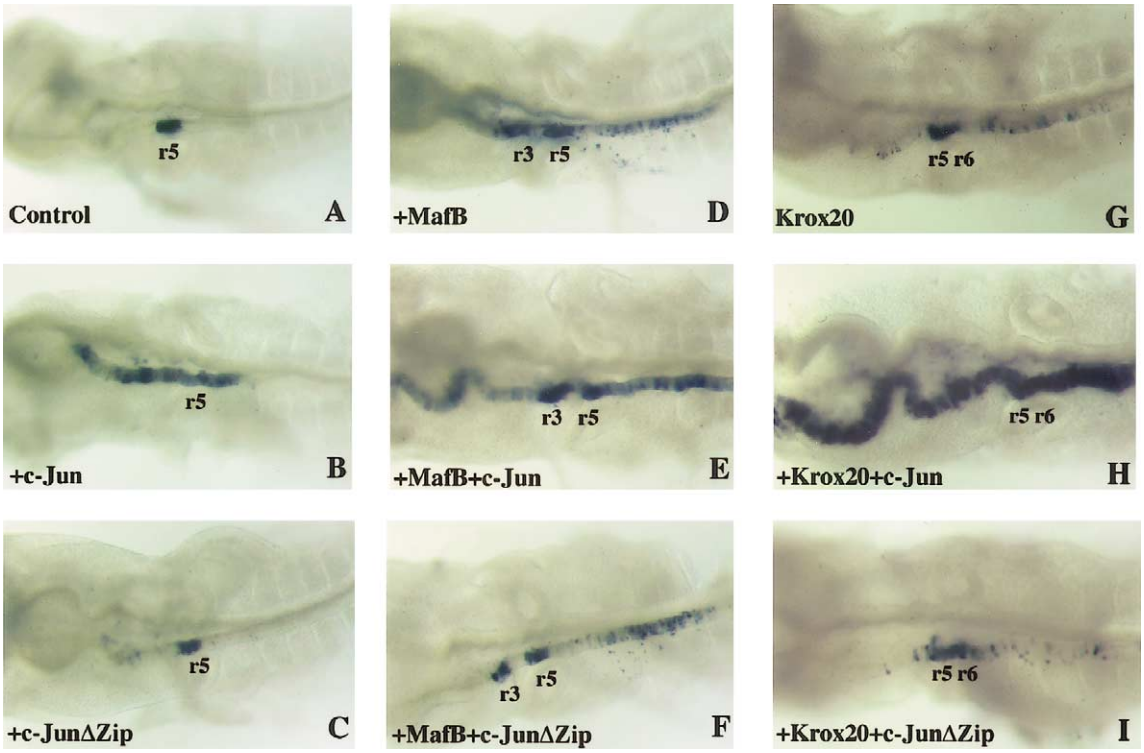

Fig. 4. c-Jun can activate the *Hoxb3* r5 enhancer and cooperate with Krox20. Chick embryos were electroporated at stages HH10-HH12 into the left side of the neural tube with a *lacZ* reporter gene driven by the human *β-globin* minimal promoter and the *Hoxb3* r5-enhancer, and Bluogal staining was performed 14 h later. The reporter construct was coelectroporated with an empty expression vector (A), a wild-type c-*jun* expression vector (B) or a construct expressing a mutated form of c-Jun deleted of the Zip domain (C, c-JunΔZip). In (D–F), coelectroporation was performed with a *MafB* expression vector together with the empty vector (D), the wild-type c-*jun* vector (E), or the c-*junΔZip* vector (F). In (G–I), coelectroporation was performed with a *Krox20* expression vector together with the empty vector (G), the wild-type c-*jun* vector (H), and the c-*junΔZip* vector (I).

transcription, suggesting that additional regulatory factors (positive or negative) are involved in the control of c-*jun* expression in r5/r6. Analysis of c-*jun cis*-acting regulatory elements will be required to further understand its transcriptional control and to identify additive *trans*-acting factors.

Complexity of Hoxb3 control in r5

We show that c-Jun is involved in the early phase of *Hoxb3* expression in r5 and that it acts through the previously identified *Hoxb3* r5 enhancer. This enhancer has been shown to carry both MafB and Krox20 binding sites that are essential for its activity (Manzanares et al., 1997, 1999b, 2002). Furthermore, MafB and Krox20 have been shown to synergistically cooperate in regulating enhancer activity and *Hoxb3* expression (Manzanares et al., 2002). The domain of *Hoxb3* expression in the hindbrain reflects these requirements, since it corresponds precisely to the intersection of the territories where MafB (r5 and r6) and Krox20 (r3 and r5) are expressed. Our data add further complexity to the regulation of *Hoxb3*, as we show that the expression of *Hoxb3* in r5 can be divided in two phases, an early phase (around 5 s stage) which is dependent on c-Jun, and a late phase (around 10–12 s stage) that is c-Jun-independent. Other AP-1 members, such as JunB and JunD, are not expressed in the hindbrain at that stage (data not shown), suggesting that they are not involved in the late upregulation of *Hoxb3* in *c-jun* mutant embryos. Moreover, it has been shown that these AP-1 members are not upregulated in the *c-jun* knock-out (Eferl et al., 1999). Our electroporation studies in chick embryos confirm and extend the mouse data. They demonstrate that c-Jun can cooperate with Krox20 in the activation of the *Hoxb3* r5-enhancer.

It is unclear why c-Jun is required for the early phase of *Hoxb3* expression, while c-*jun* is itself under the control of MafB. However, the following points are noteworthy: (1) Although one of the two MafB binding sites (the Kr2 site) in the *Hoxb3* r5 enhancer is absolutely required for activity, it interacts relatively poorly with MafB homodimers (Fig. 5C). (2) During the early phase of *Hoxb3* expression in r5, the level of MafB in this rhombomere is likely to be much lower than at later stages (judging from the levels of mRNA; Fig. 1). (3) MafB can form heterodimers with c-Jun, as shown by coimmunoprecipitations and bandshift experiments (Fig. 5A and C). On the basis of these observations, we propose the following model for *Hoxb3* regulation in r5: at the onset of *Hoxb3* expression, the level of MafB in r5 is sufficient to allow transcriptional activation of

Table 1
lacZ reporter expression in the neural tube of electroporated chick embryos

Experiment	Number of embryos	*lacZ* expression along the neural tube		
A		r5 +/− sparse X-gal-positive cells out of r5	r5 + moderate X-gal staining out of r5	r5 + strong X-gal staining out of r5
control vector	10	100%	0%	0%
c-Jun	10	30%	70%	0%
c-JunΔZip	10	100%	0%	0%
B		r3 + r5 +/− sparse X-gal-positive cells out of r3/r5	r3 + r5 + moderate X-gal staining out of r3/r5	r3 + r5 + strong X-gal staining out of r3/r5
MafB	11	63%	36%	0%
MafB + c-Jun	17	12%	88%	0%
MafB + c-JunΔZip	10	80%	20%	0%
C		r5 + r6 +/− sparse X-gal-positive cells out of r5/r6	r5 + r6 + moderate X-gal staining out of r5/r6	r5 + r6 + strong X-gal staining out of r5/r6
Krox20	4	100%	0%	0%
Krox20 + c-Jun	6	17%	33%	50%
Krox20 + c-JunΔZip	4	100%	0%	0%

Note. Consequences of c-Jun (A), MafB (B), and Krox20 (C) ectopic expression have been evaluated on the *Hoxb3*-r5 enhancer activity by following the appearance of LacZ staining. The total number of electroporated embryos in each condition is indicated as well as the percentage of X-gal-positive embryos presenting alterations in the *lacZ* pattern along the electroporated neural tube. Moderate staining corresponds to 20–50% Xgal-positive cells along the neural tube apart from the indicated rhombomeres. In strong staining embryos, the number of Xgal-positive cells outside the indicated rhombomeres reaches 60–100% of total cells.

c-*jun*, but not to sustain *Hoxb3* activation. In contrast, c-Jun itself has sufficient affinity to bind efficiently to the Kr2 site of the *Hoxb3* r5-enhancer, either as a homodimer or heterodimer with MafB, and to activate *Hoxb3* expression in r5 synergistically with Krox20. At later stages, the level of MafB in r5 increases dramatically and can replace c-Jun, either as a homodimer or a heterodimer with other bZip proteins. At this stage, c-Jun is no longer required for expression of *Hoxb3* in r5.

In conclusion, c-Jun appears to accelerate the activation of *Hoxb3* by MafB, allowing transcriptional activation when MafB alone is insufficient. In addition, the identification of c-Jun as a novel upstream regulator of *Hoxb3* supports an important role for MafB partners in hindbrain patterning. The complexity of interactions involved in this latter process may offer additional levels of regulation for fine tuning of gene expression.

The role of c-Jun during development

The delay in *Hoxb3* activation in r5 is the only phenotype that we have so far identified associated with c-*jun* inactivation at early developmental stages. The normal expression of r5 markers, such as *Hoxa3, MafB, Krox20,* and *EphA4*, indicates that the patterning of r5 and r6 is not dramatically affected and that the restored expression of *Hoxb3* in r5 at later stages does not result from a delay in maturation of this rhombomere. Furthermore, the lack of modification in the *Phox2B* and neurofilament expression patterns suggests that specification of regional identity and neurogenesis in r5 and r6 are not dramatically perturbed. *Hoxb3*$^{-/-}$ mice survive until adulthood, but show minor defects in the cervical vertebrae (Manley and Capecchi, 1997). The early lethality of the *c-jun* mutants at 13.5 dpc prevents us from determining whether the delayed expression of *Hoxb3* leads to similar defects.

Outside of the CNS, several of the early sites of c-*jun* expression are correlated with phenotypic consequences. We show that the *c-jun* gene is expressed in the foregut and the septum transversum. This latter structure is critical for liver formation as it affects the outgrowth of hepatic ducts and also influences the vascular organisation of the foregut/midgut junction (Rossi et al., 2001). The impaired hepatogenesis observed in *c-jun*$^{-/-}$ mutants might reflect a premature deficiency in the foregut and/or result from an early defect in the septum transversum. We also observed *c-jun* expression in the future sclerotomal compartment of the recently formed somites. Consistently, conditional inactivation of *c-jun* in the sclerotome and notochord has been shown to perturb the development of intervertebral bodies (Behrens et al., 2003). The demonstration of a causal link between these different sites of early *c-jun* expression and the observed phenotypes deserves further investigation.

Conclusion

Proteins of the Jun family are involved in the regulation of various cellular processes, including cell proliferation, differentiation, apoptosis, and oncogenesis. This functional versatility arises, in part, from their ability to dimerise with other bZip proteins. In this study, we have identified a role for c-Jun in the regulatory network controlling hindbrain segmentation. c-*jun* is downstream of MafB and participates together with MafB in the activation of *Hoxb3* expression.

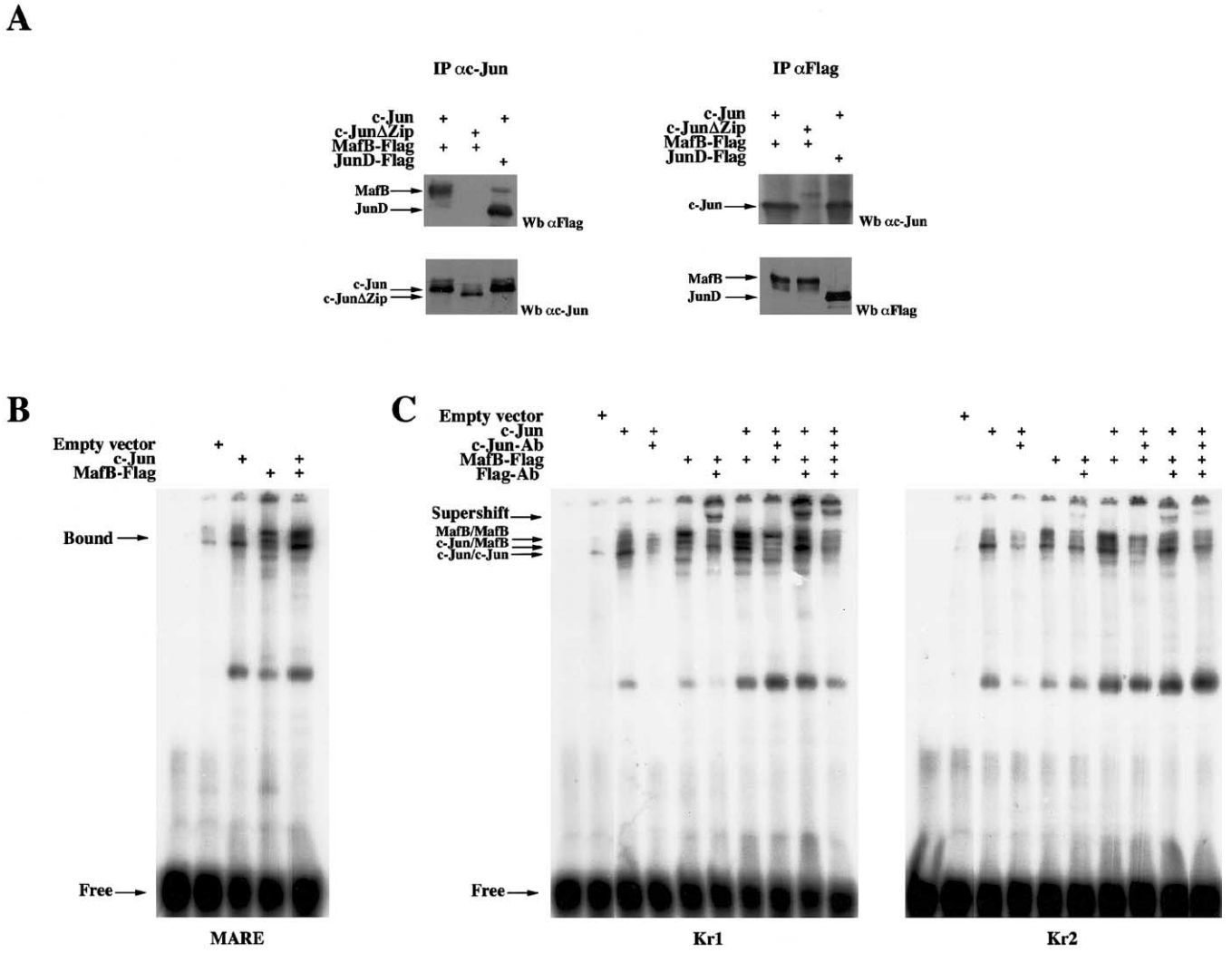

Fig. 5. c-Jun interacts with MafB and binds to the MafB/kreisler binding sites (Kr1 and Kr2) of the *Hoxb3*-r5 enhancer. (A) The plasmids encoding c-Jun or c-JunΔZip (a C-terminal truncated mutant), MafB-Flag, or JunD-Flag were cotransfected into C33A cells as indicated. The yield of transfected proteins in extracts was determined by immunoblotting with either anti-Flag or anti-c-Jun antibodies (bottom panels; Wb, Western blot). In the upper left panel, protein interactions were analysed by immunoprecipitation (IP) with an anti-c-Jun antibody followed by Western blotting with an anti-Flag monoclonal antibody. The reciprocal experiment is presented in the upper right panel: IP was performed with the anti-Flag antibody and detection of c-Jun in the Flag immunoprecipitates by using a c-Jun specific antibody. The AP-1 interacting partner, JunD, and a mutated form of c-Jun deleted of the Zip domain, c-JunΔZip, were used as positive and negative controls, respectively. (B) The consensus MARE sequence was incubated with nuclear extracts from cells transfected with c-*jun* or *MafB-Flag* expression plasmids, and the formation of protein–DNA complexes was assessed by EMSA. Equal amount of nuclear extracts were used for each line. (C) The same EMSA was performed with DNA probes carrying the Kr1 and Kr2 sequences from the *Hoxb3*-r5 enhancer. The composition of protein DNA was investigated by addition of specific anti-c-Jun or anti-Flag antibodies. The anti-Jun antibody decreases AP-1/DNA complex formation (Mechta et al., 1997), whereas the anti-Flag generates a supershifted band.

Our analysis reveals an increasing complexity of the network, which may be related to the necessity for stringent control of the accuracy of gene expression for the patterning programme. Our data also support previous observations suggesting an involvement of other bZip factors in the control of expression of MafB target genes (Manzanares et al., 2002). Further studies will be required to identify additional bZip MafB partners and to complete our understanding of their role, together with c-Jun, in the patterning events downstream of MafB.

Acknowledgments

We thank Drs. E.F. Wagner and J. Lewis for the kind gift of the *c-jun* and *kreisler* mouse lines, respectively. We thank Drs. S. Schneider-Maunoury, J.B. Weitzman, and C. Vesque for critical reading of the manuscript and Drs. S. Garel, P. Gilardi-Hebenstreit, and J. Barra for fruitful discussions. We are grateful to Drs. D. Wilkinson, G.S. Barsh, S.P. Cordes, J.F. Brunet, and C. Goridis for probes. We warmly thank Dr. S. Schneider-Maunoury for generous as-

sistance in many experimental systems and acknowledge the expert contribution of C. Lefevre and her colleagues at the ENS animal house. F.G. was supported by fellowships from MENRT, LNCC, and Institut Lilly. This work was supported by grants from INSERM, MENRT, EC, ARC, and AFM (to P.C.) and by grants from ARC, LNFCC, European Community Biomed and Training and Mobility programs (to M.Y.).

References

Alexandre, D., Clarke, J.D., Oxtoby, E., Yan, Y.L., Jowett, T., Holder, N., 1996. Ectopic expression of Hoxa-1 in the zebrafish alters the fate of the mandibular arch neural crest and phenocopies a retinoic acid-induced phenotype. Development 122, 735–746.

Angel, P., Allegretto, E.A., Okino, S.T., Hattori, K., Boyle, W.J., Hunter, T., Karin, M., 1988. Oncogene jun encodes a sequence-specific trans-activator similar to AP-1. Nature 332, 166–171.

Angel, P., Imagawa, M., Chiu, R., Stein, B., Imbra, R.J., Rahmsdorf, H.J., Jonat, C., Herrlich, P., Karin, M., 1987. Phorbol ester-inducible genes contain a common cis element recognized by a TPA-modulated trans-acting factor. Cell 49, 729–739.

Barrow, J.R., Capecchi, M.R., 1996. Targeted disruption of the Hoxb-2 locus in mice interferes with expression of Hoxb-1 and Hoxb-4. Development 122, 3817–3828.

Behrens, A., Haigh, J., F, M.-G., Dietz, U., Balling, R., Yaniv, M., Wagner, E., 2003. Impaired intervertebral discformation in the absence of c-jun. Development 130, 103–109.

Birgbauer, E., Fraser, S.E., 1994. Violation of cell lineage restriction compartments in the chick hindbrain. Development 120, 1347–1356.

Birgbauer, E., Sechrist, J., Bronner-Fraser, M., Fraser, S., 1995. Rhombomeric origin and rostrocaudal reassortment of neural crest cells revealed by intravital microscopy. Development 121, 935–945.

Bossy-Wetzel, E., Bakiri, L., Yaniv, M., 1997. Induction of apoptosis by the transcription factor c-Jun. EMBO J. 16, 1695–1709.

Cairns, B.R., Kim, Y., Sayre, M.H., Laurent, B.C., Kornberg, R.D., 1994. A Multisubuit Complex Containing the SWI1/ADR6, SW12/SNF2, SW13, SNF5, and SNF6 gene products isolated from yeast. Proc. Natl. Acad. Sci. USA 91, 1950–1954.

Clarke, J.D., Erskine, L., Lumsden, A., 1998. Differential progenitor dispersal and the spatial origin of early neurons can explain the predominance of single-phenotype clones in the chick hindbrain. Dev. Dyn. 212, 14–26.

Cordes, S.P., Barsh, G.S., 1994. The mouse segmentation gene kr encodes a novel basic domain-leucine zipper transcription factor. Cell 79, 1025–1034.

Curran, T., Franza, B.J., 1988. Fos and Jun: the AP-1 connection. Cell 55, 395–397.

Dignam, J.D., Lebovitz, R.M., Roeder, R.G., 1983. Accurate transcription initiation by RNA polymerase II in a soluble extract from isolated mammalian nuclei. Nucleic Acids Res. 11, 1475–1489.

Eferl, R., Sibilia, M., Hilberg, F., Fuchsbichler, A., Kufferath, I., Guertl, B., Zenz, R., Wagner, E.F., Zatloukal, K., 1999. Functions of c-Jun in liver and heart development. J. Cell Biol. 145, 1049–1061.

Eichmann, A., Grapin-Botton, A., Kelly, L., Graf, T., Le Douarin, N.M., Sieweke, M., 1997. The expression pattern of the mafB/kr gene in birds and mice reveals that the kreisler phenotype does not represent a null mutant. Mech. Dev. 65, 111–122.

Fraser, S., Keynes, R., Lumsden, A., 1990. Segmentation in the chick embryo hindbrain is defined by cell lineage restrictions. Nature 344, 431–435.

Frohman, M.A., Martin, G.R., Cordes, S.P., Halamek, L.P., Barsh, G.S., 1993. Altered rhombomere-specific gene expression and hyoid bone differentiation in the mouse segmentation mutant, kreisler (kr). Development 117, 925–936.

Gavalas, A., Davenne, M., Lumsden, A., Chambon, P., Rijli, F.M., 1997. Role of Hoxa-2 in axon pathfinding and rostral hindbrain patterning. Development 124, 3693–3702.

Gendron-Maguire, M., Mallo, M., Zhang, M., Gridley, T., 1993. Hoxa-2 mutant mice exhibit homeotic transformation of skeletal elements derived from cranial neural crest. Cell 75, 1317–1331.

Ghislain, J., Desmarquet-Trin-Dinh, C., Gilardi-hebenstreit, P., Charnay, P., Frain, M., 2003. Neural crest patterning: autoregulatory and crest specific elements cooperate for Krox-20 transcriptional control. Development 130, 941–953.

Giudicelli, F., Taillebourg, E., Charnay, P., Gilardi-Hebenstreit, P., 2001. Krox-20 patterns the hindbrain through both cell-autonomous and non cell-autonomous mechanisms. Genes Dev. 15, 567–580.

Giudicelli, F., Gilardi-Hebenstreit, P., Mechta-Grigoriou, F., Poquet, C., Charnay, P., 2003. Novel abnormalities of MafB underlie its individual role in hindbrain segmentation and regional specification. Dev. Biol. 253, 150–162.

Goddard, J.M., Rossel, M., Manley, N.R., Capecchi, M.R., 1996. Mice with targeted disruption of Hoxb-1 fail to form the motor nucleus of the VIIth nerve. Development 122, 3217–3228.

Halazonetis, T.D., Georgopoulos, K., Greenberg, M.E., Leder, P., 1988. c-Jun dimerizes with itself and with c-Fos, forming complexes of different DNA binding affinities. Cell 55, 917–924.

Helmbacher, F., Pujades, C., Desmarquet, C., Frain, M., Rijli, F.M., Chambon, P., Charnay, P., 1998. Hoxal and Krox-20 synergize to control the development of rhombomere 3. Development 125, 4739–4748.

Hilberg, F., Aguzzi, A., Howells, N., Wagner, E.F., 1993. c-jun is essential for normal mouse development and hepatogenesis. Nature 365, 179–181.

Hirai, S.I., Ryseck, R.P., Mechta, F., Bravo, R., Yaniv, M., 1989. Characterization of junD: a new member of the jun proto-oncogene family. EMBO J. 8, 1433–1439.

Hirai, S.-I., Bourachot, B., Yaniv, M., 1990. Both Jun and Fos contribute to transcription activation by the heterodimer. Oncogene 5, 39–46.

Hunt, P., Gulisano, M., Cook, M., Sham, M.H., Faiella, A., Wilkinson, D., Boncinelli, E., Krumlauf, R., 1991. A distinct Hox code for the branchial region of the vertebrate head. Nature 353, 861–864.

Jacquin, T.D., Borday, V., Schneider-Maunoury, S., Topilko, P., Ghilini, G., Kato, F., Charnay, P., Champagnat, J., 1996. Reorganization of pontine rhythmogenic neuronal networks in Krox-20 knockout mice. Neuron 17, 747–758.

Johnson, R.S., van, L.B., Papaioannou, V.E., Spiegelman, B.M., 1993. A null mutation at the c-jun locus causes embryonic lethality and retarded cell growth in culture. Genes Dev. 7, 1309–1317.

Kataoka, K., Nishizawa, M., Kawai, S., 1993. Structure-function analysis of the maf oncogene product, a member of the b-Zip protein family. J. Virol. 67, 2133–2141.

Kataoka, K., Fujiwara, K.T., Noda, M., Nishizawa, M., 1994a. MafB, a new Maf family transcription activator that can associate with Maf and Fos but not with Jun. Mol. Cell. Biol. 14, 7581–7591.

Kataoka, K., Noda, M., Nishizawa, M., 1994b. Maf nuclear oncoprotein recognizes sequences related to an AP-1 site and forms heterodimers with both Fos and Jun. Mol. Cell. Biol. 14, 700–712.

Kerppola, T.K., Curran, T., 1994. Maf and Nrl can bind to AP-1 sites and form heterodimers with Fos and Jun. Oncogene 9, 675–684.

Kulesa, P.M., Fraser, S.E., 2000. In ovo time-lapse analysis of chick hindbrain neural crest cell migration shows cell interactions during migration to the branchial arches. Development 127, 1161–1172.

Lumsden, A., Keynes, R., 1989. Segmental patterns of neuronal development in the chick hindbrain. Nature 337, 424–428.

Lumsden, A., Sprawson, N., Graham, A., 1991. Segmental origin and migration of neural crest cells in the hindbrain region of the chick embryo. Development 113, 1281–1291.

Lumsden, A., Krumlauf, R., 1996. Patterning the vertebrate neuraxis. Science 274, 1109–1115.

Manley, N.R., Capecchi, M.R., 1997. Hox group 3 paralogous genes act synergistically in the formation of somitic and neural crest-derived structures. Dev. Biol. 192, 274–288.

Manzanares, M., Cordes, S., Kwan, C.T., Sham, M.H., Barsh, G.S., Krumlauf, R., 1997. Segmental regulation of Hoxb-3 by kreisler. Nature 387, 191–195.

Manzanares, M., Cordes, S., Ariza-McNaughton, L., Sadl, V., Maruthainar, K., Barsh, G., Krumlauf, R., 1999a. Conserved and distinct roles of kreisler in regulation of the paralogous Hoxa3 and Hoxb3 genes. Development 126, 759–769.

Manzanares, M., Trainor, P.A., Nonchev, S., Ariza-McNaughton, L., Brodie, J., Gould, A., Marshall, H., Morrison, A., Kwan, C.T., Sham, M.H., Wilkinson, D.G., Krumlauf, R., 1999b. The role of kreisler in segmentation during hindbrain development. Dev. Biol. 211, 220–237.

Manzanares, M., Bel-Vialar, S., Ariza-McNaughton, L., Ferretti, E., Marshall, H., Maconochie, M.M., Blasi, F., Krumlauf, R., 2001. Independent regulation of initiation and maintenance phases of Hoxa3 expression in the vertebrate hindbrain involve auto- and cross-regulatory mechanisms. Development 128, 3595–3607.

Manzanares, M., Nardelli, J., Gilardi-Hebenstreit, P., Marshall, H., Giudicelli, F., Martinez-Pastor, M.T., Krumlauf, R., Charnay, P., 2002. Krox-20 and Kreisler co-operate in the transcriptional control of segmental expression of Hoxb3 in the developing hindbrain. EMBO 21, 365–376.

McKay, I.J., Muchamore, I., Krumlauf, R., Maden, M., Lumsden, A., Lewis, J., 1994. The kreisler mouse: a hindbrain segmentation mutant that lacks two rhombomeres. Development 120, 2199–2211.

Mechta, F., Lallemand, D., Pfarr, C.M., Yaniv, M., 1997. Transformation by ras modifies AP1 composition and activity. Oncogene 14, 837–847.

Mechta-Grigoriou, F., Gerald, D., Yaniv, M., 2001. The mammalian Jun proteins: redundancy and specificity. Oncogene 20, 2378–2389.

Nonchev, S., Vesque, C., Maconochie, M., Seitanidou, T., Ariza-McNaughton, L., Frain, M., Marshall, H., Sham, M.H., Krumlauf, R., Charnay, P., 1996. Segmental expression of Hoxa-2 in the hindbrain is directly regulated by Krox-20. Development 122, 543–554.

Osumi-Yamashita, N., Ninomiya, Y., Doi, H., Eto, K., 1996. Rhombomere formation and hindbrain crest cell migration from prorhombomeric origins in mouse embryos. Dev. Growth Differ. 38, 107–118.

Pattyn, A., Morin, X., Cremer, H., Goridis, C., Brunet, J.F., 1997. Expression and interactions of the two closely related homeobox genes Phox2a and Phox2b during neurogenesis. Development 124, 4065–4075.

Pfarr, C.M., Mechta, F., Spyrou, G., Lallemand, D., Carillo, S., Yaniv, M., 1994. Mouse JunD negatively regulates fibroblast growth and antagonizes transformation by ras. Cell 76, 747–760.

Rijli, F.M., Gavalas, A., Chambon, P., 1998. Segmentation and specification in the branchial region of the head: the role of the Hox selector genes. Int. J. Dev. Biol. 42, 393–401.

Rijli, F.M., Mark, M., Lakkaraju, S., Dierich, A., Dolle, P., Chambon, P., 1993. A homeotic transformation is generated in the rostral branchial region of the head by disruption of Hoxa-2, which acts as a selector gene. Cell 75, 1333–1349.

Rossi, J.M., Dunn, N.R., Hogan, B.L., Zaret, K.S., 2001. Distinct mesodermal signals, including BMPs from the septum transversum mesenchyme, are required in combination for hepatogenesis from the endoderm. Genes Dev. 15, 1998–2009.

Ruberte, E., Wood, H., Morris-Kay, G., 1997. Prorhombomeric subdivision of the mammalian embryonic hindbrain: is it functionally meaningful? Int. J. Dev. Biol. 41, 213–222.

Sassone-Corsi, P., Lamph, W.W., Kamps, M., Verma, I.M., 1988. fos-associated cellular p39 is related to nuclear transcription factor AP-1. Cell 54, 553–560.

Schneider-Maunoury, S., Topilko, P., Seitandou, T., Levi, G., Cohen-Tannoudji, M., Pournin, S., Babinet, C., Charnay, P., 1993. Disruption of Krox-20 results in alteration of rhombomeres 3 and 5 in the developing hindbrain. Cell 75, 1199–1214.

Schneider-Maunoury, S., Seitanidou, T., Charnay, P., Lumsden, A., 1997. Segmental and neuronal architecture of the hindbrain of Krox-20 mouse mutants. Development 124, 1215–1226.

Schneider-Maunoury, S., Gilardi-Hebenstreit, P., Charnay, P., 1998. How to build a vertebrate hindbrain. Lessons from genetics. C. R. Acad. Sci. III 321, 819–834.

Seitanidou, T., Schneider-Maunoury, S., Desmarquet, C., Wilkinson, D.G., Charnay, P., 1997. Krox-20 is a key regulator of rhombomere-specific gene expression in the developing hindbrain. Mech. Dev. 65, 31–42.

Serbedzija, G.N., Bronner-Fraser, M., Fraser, S.E., 1992. Vital dye analysis of cranial neural crest cell migration in the mouse embryo. Development 116, 297–307.

Sham, M.H., Hunt, P., Nonchev, S., Papalopulu, N., Graham, A., Boncinelli, E., Krumlauf, R., 1992. Analysis of the murine Hox-2.7 gene: conserved alternative transcripts with differential distributions in the nervous system and the potential for shared regulatory regions. EMBO J. 11, 1825–1836.

Sham, M.H., Vesque, C., Nonchev, S., Marshall, H., Frain, M., Gupta, R.D., Whiting, J., Wilkinson, D., Charnay, P., Krumlauf, R., 1993. The zinc finger gene Krox20 regulates HoxB2, (Hox2.8) during hindbrain segmentation. Cell 72, 183–196.

Studer, M., Lumsden, A., Ariza-McNaughton, L., Bradley, A., Krumlauf, R., 1996. Altered segmental identity and abnormal migration of motor neurons in mice lacking Hoxb-1. Nature 384, 630–634.

Swiatek, P.J., Gridley, T., 1993. Perinatal lethality and defects in hindbrain development in mice homozygous for a targeted mutation of the zinc finger gene Krox-20. Genes Dev. 7, 2071–2084.

Trainor, P.A., Krumlauf, R., 2000. Patterning the cranial neural crest: hindbrain segmentation and Hox gene plasticity. Nat. Rev. Neurosci. 1, 116–124.

Trainor, P.A., Sobieszczuk, D., Wilkinson, D., Krumlauf, R., 2002. Signalling between the hindbrain and paraxial tissues dictates neural crest migration pathways. Development 129, 433–442.

Voiculescu, O., Taillebourg, E., Pujades, C., Kress, C., Buart, S., Charnay, P., Schneider-Maunoury, S., 2001. Hindbrain patterning: Krox20 couples segmentation and specification of regional identity. Development 128, 4967–4978.

Wigler, M., Silverstein, S., Lee, L.S., Pellicer, A., Cheng, Y.C., Axel, R., 1977. Transfer of purified herpes virus thymidine kinase related gene to cultured mouse cells. Cell 11, 223–232.

Wilkinson, D.G., Bhatt, S., Chavrier, P., Bravo, R., Charnay, P., 1989a. Segment-specific expression of a zinc-finger gene in the developing nervous system of the mouse. Nature 337, 461–464.

Wilkinson, D.G., Bhatt, S., Cook, M., Boncinelli, E., Krumlauf, R., 1989b. Segmental expression of Hox-2 homoeobox-containing genes in the developing mouse hindbrain. Nature 341, 405–409.

Wilkinson, D.G., Bhatt, S., Ryseck, R.P., Bravo, R., 1989b. Tissue-specific expression of c-jun and junB during organogenesis in the mouse. Development 106, 465–471.

Wilkinson, D.G., Nieto, M.A., 1993. Detection of messenger RNA by in situ hybridization to tissue sections and whole mounts. Methods Enzymol. 225, 361–373.

Wingate, R.J., Lumsden, A., 1996. Persistence of rhombomeric organisation in the postsegmental hindbrain. Development 122, 2143–2152.

Zhang, M., Kim, H.J., Marshall, H., Gendron-Maguire, M., Lucas, D.A., Baron, A., Gudas, L.J., Gridley, T., Krumlauf, R., Grippo, J.F., 1994. Ectopic Hoxa-1 induces rhombomere transformation in mouse hindbrain. Development 120, 2431–2442.